



ACADEMIC  
PRESS

Available online at [www.sciencedirect.com](http://www.sciencedirect.com)

SCIENCE @ DIRECT®

Journal of Sound and Vibration 266 (2003) 481–491

---

---

JOURNAL OF  
SOUND AND  
VIBRATION

---

---

[www.elsevier.com/locate/jsvi](http://www.elsevier.com/locate/jsvi)

# A multibody dynamic approach for colliding particles

K. van Staeyen, E. Tijskens\*, H. Ramon

*Department of Agro-Engineering and -Economics, Laboratory for Agro-Machinery and Processing,  
Catholic University Leuven, Kasteelpark Arenberg 30, 3001 Leuven, Belgium*

Received 13 January 2003

---

## Abstract

The dynamics of systems of moving particles in engineering applications is rapidly gaining interest as the incentive to control and optimize granular flow systems increases. Increasing availability of computing power has rendered the *in silico* study of large assemblies of discrete particles in near-realistic systems feasible. Generally, the governing equations for systems of non-adhesive discrete particles are derived from Newton's equation of motion with the basic assumption that the normal and tangential forces arising between two impacting particles can be independently derived from the virtual overlap of the particles and the tangential displacement of the initial contact points. In this study, the problem is placed in a rigorous multibody dynamics setting and a detailed comparison is made with the classical theory. An attempt has been made to treat particles and walls in a unified way.

© 2003 Elsevier Ltd. All rights reserved.

---

## 1. Introduction

Multibody dynamics is an integrated approach to describe and predict the motion of complex multibody systems as a reaction to internal or external forces acting on the system. Multibody dynamics has been thoroughly elaborated and all kinds of mechanisms have been described using this theory [1]. Discrete element method (DEM) simulations however have always used the Newton–Euler method to describe the motion of the particles involved. This is explained by the fact that until now most simulations used very simple geometric forms (circles, ellipses, or polygons) and were carried out in two dimensions. Recently, DEM modellers started to simulate the behaviour of more complex forms in three dimensions [2,3]. Of course, DE particles will never be connected to each other in the sense of a multibody system, therefore the full range of possibilities of multibody dynamics cannot be used in DEM. In this paper multibody dynamics

---

\*Corresponding author. Tel.: +32-16-32-8595; fax: +32-16-32-8590.

*E-mail address:* [engelbert.tijskens@agr.kuleuven.ac.be](mailto:engelbert.tijskens@agr.kuleuven.ac.be) (E. Tijskens).

will be used to describe the interactions between colliding particles and to derive the equations of motion of the particles. A comparison is made with the Newton–Euler method. Further, an attempt has been made to describe a particle–wall interaction and to calculate the equations of motion for this case using exactly the same method.

## 2. Equations of motion in multibody dynamics

The equations of motion can be derived using the Newton–Euler method. However in multibody dynamics the use of Lagrange’s equation combined with the principle of virtual work is a more common method [4]:

$$\frac{d}{dt} \left( \frac{\partial T}{\partial \dot{\mathbf{q}}} \right) - \frac{\partial T}{\partial \mathbf{q}} = \mathbf{f}, \quad (1)$$

One can think of Lagrange’s equation as a ‘balance of motional forces’. On the left side the ‘outputs’, the effects on the motion, on the right side the ‘inputs’, the forces  $\mathbf{f}$  that have established this effect. In this equation  $T$  is the kinetic energy of the system and  $\mathbf{q}$  stands for the ‘*generalized co-ordinate*’ vector, consisting of the directions along which motion of the system is possible, considering all its constraints. Using this generalized co-ordinate, the virtual work for internal and external forces can be calculated.

External forces are not influenced by the motion of the multibody system. Internal forces, on the contrary, arise from the interactions between the parts of the multibody system; the magnitude of their force vector is unknown in advance and is calculated as

$$F = k\|\mathbf{l}\| + c\|\dot{\mathbf{l}}\| + f. \quad (2)$$

The length of the connecting vector between the two bodies is represented by  $\|\mathbf{l}\|$ ,  $k$  and  $c$  are spring and damper constants and  $f$  is the magnitude of an actuator force, which is not present in the DEM. In most DE models, gravity is the only external force. Particle interactions, with another particle as well as with a boundary, can be seen as internal forces: their magnitude depends on the interaction itself. This means they are an essential part of the dynamics of a two-particle system.

### 2.1. Frames of references

Multibody dynamics uses a distinct reference frame for each separately moving part of a body. In this paper four different frames of reference will be used:  $\mathbf{Q}_0$ , the inertial frame,  $\mathbf{Q}_1$  and  $\mathbf{Q}_2$ , the frames fixed to their respective particles, with their centres located at the centre of mass of the respective particles. And finally  $\mathbf{Q}_3$ , the collision reference—a frame, with its centre located at the centre of mass of particle 1 and its unit vector  ${}^3\mathbf{e}_x$  always pointing to the centre of mass of particle 2 (Fig. 1). All reference frames are Cartesian and right handed; all unit vectors have the same length.

Now a vector  $\mathbf{v}$  can be expressed in a reference frame  $\mathbf{Q}_i$  as  ${}^i\mathbf{v}$ . To find the algebraic notation of these vectors in another reference frame  $\mathbf{Q}_j$  a transformation matrix  ${}^j\mathbf{A}_i$  is used:  ${}^j\mathbf{v} = {}^j\mathbf{A}_i {}^i\mathbf{v}$ . Taking all this information into account Lagrange’s two-dimensional equation for particle 1 in

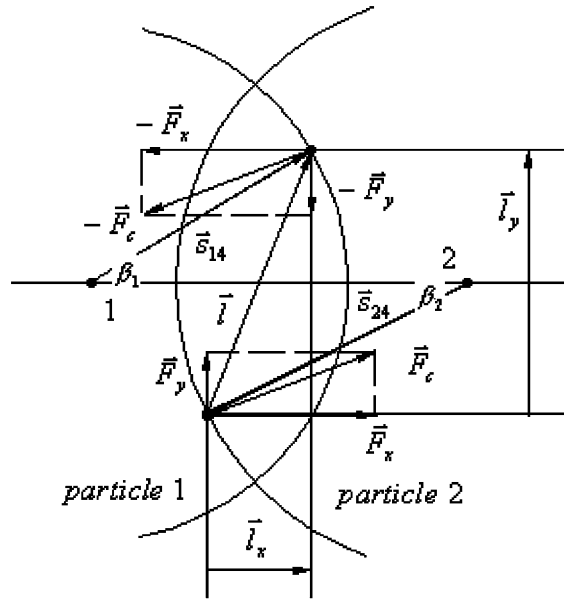


Fig. 1. The particle–particle interaction.

interaction with particle 2 can be written as [5]

$$\begin{bmatrix} m_1 & 0 & 0 \\ 0 & m_1 & 0 \\ 0 & 0 & I_1 \end{bmatrix} \begin{bmatrix} \ddot{x}_1 \\ \ddot{y}_1 \\ \ddot{\alpha}_1 \end{bmatrix} = \begin{bmatrix} 0 \\ -m_1 g \\ 0 \end{bmatrix} - {}^0\mathbf{L}_1 {}^3\mathbf{F}^i, \quad (3)$$

where  $x$  and  $y$  are the translational and  $\alpha$  the rotational degrees of freedom.  $m_1$  and  $I_1$  are the mass and inertia of particle 1 and  $g$  is the gravitational acceleration. Notice that the force effect  ${}^0\mathbf{L}_1$  is given in the inertial reference frame and the force itself  ${}^3\mathbf{F}^i$  in the reference frame of the interaction.

### 2.2. Description of the contact-vector

Just like in multibody dynamics a connecting vector is used to calculate internal forces. There is, however, an important difference: because in DEM the normal and tangential force models need not be equal, this vector’s length will not be used to derive a total interaction force, but its normal and tangential components to derive the normal and tangential interaction forces. In fact, the following equations are valid (when supposing a simple spring–damper model in the normal direction and a simple spring model in the tangential direction, where the magnitude of the tangential force is limited by a sliding element, more complex force models can easily be implemented):

$${}^3F_x = k_x {}^3l_x + v_x {}^3\dot{l}_x, \quad {}^3F_y = k_y {}^3l_y. \quad (4)$$

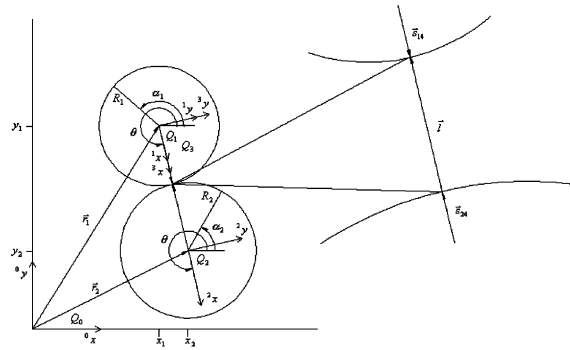


Fig. 2. The contact-vector, I.

The contact-vector  $\mathbf{l}$  connects the ‘virtual initial contact point’ on particle 2 with that on particle 1 in a two-particle system (Fig. 2). These points are the first to establish contact between the two particles. Due to the allowed ‘overlap’ in the DEM their positions become virtual.

Using this contact-vector allows one to calculate normal and tangential forces as well as their effects on the motion of the particles involved from one single vector and its derivatives! Computations can be done on a more abstract level, giving fewer opportunities for errors to occur. Errors that do occur will have an effect on the whole system’s dynamics at once and will not remain unnoticed. The contact-vector can be found as

$$\mathbf{l} = -\mathbf{s}_{24} - \mathbf{r}_2 + \mathbf{r}_1 + \mathbf{s}_{14}. \tag{5}$$

Using the transformation of reference frames the contact vector can be written as

$${}^0\mathbf{l} = -{}^0\mathbf{A}_2{}^2\mathbf{s}_{24} - ({}^0\mathbf{r}_2 - {}^0\mathbf{r}_1) + {}^0\mathbf{A}_1{}^1\mathbf{s}_{14}. \tag{6}$$

This can clearly be seen in Fig. 2.

Using this contact-vector as well as its time derivative projected in the interaction reference frame allows one to determine the normal and tangential forces in this reference frame.

Expressing the virtual displacement of the contact-vector—a displacement, which is possible given the constraints of the system—in terms of the generalised co-ordinates shows that  ${}^0\mathbf{L}_1$  is the motional effect of this force:

$${}^0\mathbf{L}_1 = \begin{bmatrix} \cos \theta - \frac{RSIN}{d_{12}} \sin \theta & -\frac{RCOS}{d_{12}} \sin \theta \\ \sin \theta + \frac{RSIN}{d_{12}} \cos \theta & \frac{RCOS}{d_{12}} \cos \theta \\ R_1 \sin \beta_1 & R_1 \cos \beta_1 \end{bmatrix}, \tag{7}$$

where

$$RSIN = R_1 \sin \beta_1 + R_2 \sin \beta_2, \tag{8}$$

$$RCOS = R_1 \cos \beta_1 + R_2 \cos \beta_2 \tag{9}$$

and

$$d_{12} = |\mathbf{x}_j - \mathbf{x}_i|. \tag{10}$$

The *RSIN* and *RCOS* terms describe the effects of the displacements of the particles' centres of mass on the interaction frame. Their individual effect, however, is not fully understood. Understanding this effect requires a lot of spatial insight. Notice that  ${}^0\mathbf{L}_1$  gives the effect on the particle motion directly in the inertial reference frame. In the calculations of  ${}^0\mathbf{L}_1$  it can clearly be seen that a rotation from the inertial frame to the interaction frame must be incorporated. In a simple case like this the force's effects are obvious and the Newton–Euler method may be a lot faster and easier. However in more complex situations this method requires lots of spatial insights and a very attentive working style, while calculating  ${}^0\mathbf{L}_1$  remains a straightforward, simple work.

At this point Lagrange's equation (1) can be filled in with the contact-vector and its derivatives to calculate the equations of motion. This can be done by a computer.

### 3. Comparison with the Newton–Euler approach

To check these theoretical results they have been compared with the corresponding variables used in Refs. [6,7]. First of all the overlap has been defined as

$$\Delta_{12} = (r_2 + r_1) - |\mathbf{x}_2 - \mathbf{x}_1| \geq 0 \tag{11}$$

and the relative velocity of particle *j* with respect to particle *i* at the point of contact will be calculated as

$$\delta\dot{\mathbf{x}}_{12} = \dot{\mathbf{x}}_2 - \dot{\mathbf{x}}_1 - (\dot{\alpha}_2 R_2 + \dot{\alpha}_1 R_1)\hat{\mathbf{s}}_{12}, \tag{12}$$

where  $\hat{\mathbf{n}}_{12}$  is the normal and  $\hat{\mathbf{s}}_{12}$  the tangential unit vector. This formula refers to the situation depicted in Fig. 3. Notice the difference with Fig. 1, where the effect of the overlap and the virtual tangential displacement are also taken into account. The normal force can now be calculated as

$$\mathbf{F}_{n12} = (-k_n \Delta_{12} + v_n \delta\dot{\mathbf{x}}_{12} \cdot \hat{\mathbf{n}})\hat{\mathbf{n}}. \tag{13}$$

To find the tangential force the virtual tangential displacement must be calculated first:

$$\delta s_{12}(t) = \int_{t_0}^t (\delta\dot{\mathbf{x}}_{12} \cdot \hat{\mathbf{s}}_{12}) dt'. \tag{14}$$

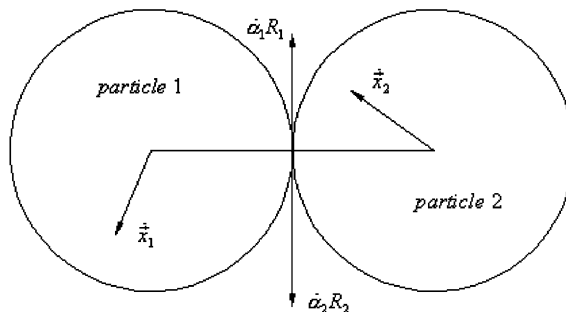


Fig. 3. Interaction of two particles.

Now the tangential force is simply

$$\mathbf{F}_{s, spring} = (k_s \delta s_{12}) \hat{\mathbf{s}}_{12}. \tag{15}$$

The magnitude of the tangential force is limited by a sliding element.

Before starting a comparison the assumption is made that overlaps are very small ( $\Delta_{12} \leq 1\%$  of the particle radius) and therefore the angle between the particle’s reference frame and the collision reference frame,  $\beta$  (Fig. 1), remains negligibly small:

$$\sin(\beta) = \beta, \quad \cos(\beta) = 1. \tag{16}$$

### 3.1. Comparing vector components

Taking this assumption into account it is easy to show that the normal component of the contact-vector (6) equals the overlap between the two particles.

$${}^3l_x = \Delta_{12}. \tag{17}$$

Comparing the time derivative of the contact-vector with  $\delta \dot{\mathbf{x}}_{12}$ , shows that

$$\mathbf{i} + {}^3\mathbf{e}^T \begin{bmatrix} \dot{\alpha}_1 R_1 \sin \beta_1 + \dot{\alpha}_2 R_2 \sin \beta_2 \\ 0 \end{bmatrix} = -\delta \dot{\mathbf{x}}_{12}. \tag{18}$$

The minus sign comes from the definition of the contact-vector in Section 2.1 (1 relative to 2) and the definition of  $\delta \dot{\mathbf{x}}_{12}$  in Section 3.1 (2 (*j*) relative to 1 (*i*)). The remaining difference is the small effect of the particle rotation ( $\dot{\alpha}$ ) on the distance to the centreline ( $R \sin \beta$ ) of the end points of the contact-vector. This effect has the same direction as the centreline of the two-particle system and therefore shows up only in the normal component when projected in  $\mathbf{Q}_3$ . Finally, the tangential component of the contact-vector is compared with the tangential displacement  $\delta s_{12}$ .

$${}^3l_y + \int_{t_0}^t {}^3l_x \dot{\theta} dt = -\delta s_{12}(t). \tag{19}$$

Here the difference is—again—the minus sign and the contribution of the rotational velocity of the overlap to the tangential displacement. Whereas the difference in Eq. (15) is negligible, this should not always be the case for Eq. (16).

These differences need not necessarily be of concern. What is really important is that the forces used in the equations of motion are exactly the same. So these forces are examined first.

### 3.2. Comparing forces

Before comparing the respective forces, one must make an important observation:

$${}^3(\dot{l}) = \dot{\theta} \begin{bmatrix} 0 & -1 \\ 1 & 0 \end{bmatrix} {}^3l + {}^3\dot{l} = \begin{bmatrix} -\dot{\theta} {}^3l_y \\ \dot{\theta} {}^3l_x \end{bmatrix} + {}^3\dot{l}, \tag{20}$$

which means that the time derivative of a vector consists of two parts: the derivative of this vector in its frame and the vector itself times the derivative of that reference frame. This is clearly

explained in Ref. [3]. Transforming (10) to the present notation would yield

$$\mathbf{F}_{n12} = (-k_x {}^3l_x - v_x {}^3\dot{l}_x) {}^3\mathbf{e}_x, \tag{21}$$

because of the negligible difference in Eq. (15). In combination with Eq. (17) this gives

$$\mathbf{F}_{n12} = -(k_x {}^3l_x + v_x({}^3l_y\dot{\theta} - {}^3\dot{l}_x)) {}^3\mathbf{e}_x, \tag{22}$$

which—except from the minus sign—shows a clear difference with Eq. (4). When transforming Eq. (12) in the same way, using Eqs. (11) and (16) one finds

$$\mathbf{F}_{s12} = -k_s \left( \int_{t_0}^t ({}^3\dot{l}_y + {}^3l_x\dot{\theta}) dt \right) {}^3\mathbf{e}_y \tag{23}$$

or

$$\mathbf{F}_{s12} = -k_s \left( {}^3l_y + \int_{t_0}^t {}^3l_x\dot{\theta} dt \right) {}^3\mathbf{e}_y. \tag{24}$$

Again this equation shows a sign and a non-negligible term as differences with Eq. (4). Compare both Eqs. (19) and (21) with Eq. (17).

### 3.3. Different forces in a special case

When imagining a situation as pictured in Fig. 3, where both  $\beta_1, \beta_2$  and the overlap are zero one finds no differences at all between the two approaches. One also notices that in this situation the length of the contact-vector is zero, and therefore also all of its components, see Eq. (17). But if one supposes a non-zero length of the contact-vector, as is the case in Fig. 1, the differences described above will be found. To find out which approach is the best suited to describe this situation, the following thought experiment will be conducted. Imagine the unusual situation in which two identical particles are held in contact by some external force or structure in a fixed position relative to each other, having a certain overlap and a certain tangential displacement (Fig. 4). This implies that the interaction forces, projected onto the interaction frame, must also be

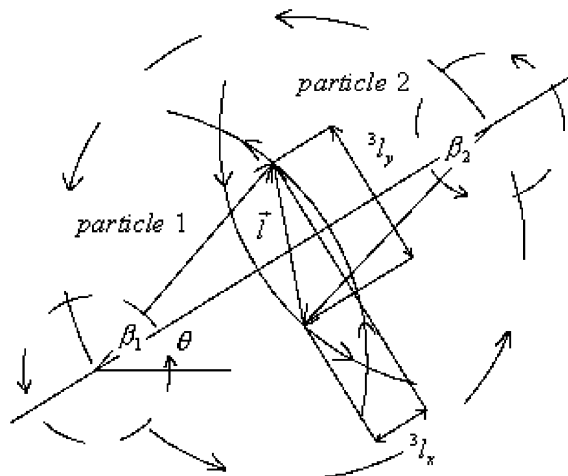


Fig. 4. Thought experiment.

constant over time. Now rotate this system. It is clear that the relative positions of the particles as seen in the interaction frame still will not change.

Therefore the interaction forces too must remain constant when projected in the interaction reference frame. When considering Eq. (4) one finds that the overlap and tangential displacement are both constant, i.e., the time derivatives of the components of  ${}^3l$  are zero. This means that in this case the components of  ${}^3F$  will be constant. However, when looking at Eq. (21) one finds a non-zero term in the integral, which—with ongoing time—will give a non-constant  ${}^3F_{s12}$ . When keeping the same configuration, but now accelerating the rotation of the system, it is found that even  ${}^3F_{n12}$  is not constant anymore, because of the non-constant rotational velocity in Eq. (19). These findings are contradictory to the principle that interaction forces should only depend on relative positions and velocities of the particles in contact. Problems arise from the fact that the relative velocity *at the point of contact* can be projected in any reference frame without problems, this means as long as the two contact-points are on the same spot. But as soon as they separate, there exists a difference between the projection of the difference of their velocities relative to the inertial frame ( $\delta\dot{\mathbf{x}}_{12} \cdot \hat{\mathbf{n}}_{12}$  or  ${}^3\dot{\mathbf{l}}$ ) and the time derivative of the projection of their relative position vector ( ${}^3\dot{\mathbf{l}}$ ), see Eq. (17). The difference one gets equals the distance between the contact points times the rotational velocity of the system. If one agrees that the motion of the system as a whole will not influence the interaction of the considered particles, one must choose the latter option to calculate the interaction forces.

### 3.4. Importance

Now that a difference has been found to exist one would like to know what is the importance of this difference in the DEM application. In the standard approach no interaction vector is used and the tangential force is mostly calculated as an incremental force. This means that an equivalent multibody approach would always have its contact-vector aligned with the normal axis of the interaction frame. In that case  ${}^3l_y$  is zero and the normal force will not show any difference. So only the tangential force will show a difference. If this difference is important or not depends on the ratio of  ${}^3l_x\dot{\theta}$  to  ${}^3\dot{l}_y$ , see Eq. (20). When comparing these two variables one finds that

$${}^3\dot{l}_y = -\dot{\theta}(R_1 + R_2) + (\dot{\alpha}_1 R_1 + \dot{\alpha}_2 R_2). \quad (25)$$

Assuming the same rotational velocity for the particles:

$${}^3\dot{l}_y = (\dot{\alpha} - \dot{\theta}) \cdot (R_1 + R_2). \quad (26)$$

When the maximum allowable overlap ( ${}^3l_x$ ) is about 1% of the particle's radius this means that  $\dot{\theta}{}^3l_x$  will only be of importance when the difference between the rotational speeds of the particles and the interaction system is about this 1%. Therefore it is believed that in most cases this difference will be negligible. Unfortunately, time has been too short to perform computer simulations using both methods to quantify this difference.

Finally, other differences could show up when using more complex force models. At the moment this is not clear yet, but possible differences are expected to be negligible as well.



#### 4. Boundaries: strange particles?

In this study it is shown that the equations of motion of a particle–fixed wall interaction can be written as a special case of a particle–particle interaction. Assuming that the strange particle is (1) at rest at  $t_0$ , has (2) an infinite radius and (3) a constant density, it is known that this particle has an infinite inertia and therefore will remain at rest. Further, assuming the position and orientation of the boundary to be known, it can easily be shown that the contact-vector in this special case equals the contact-vector for the particle–particle interaction. Indeed, it is shown that interaction with an infinitely large, non-moving particle leads to a non-rotating interaction reference frame, which allows one to simplify the contact-vector for this case. Filling in the assumptions then brings the final conclusion.

##### 4.1. Implementation

The aim in treating boundaries as particles was to allow the construction of a generic program in which confining geometry with moving parts can be incorporated without difficulty and in which particles and walls can be treated in a unified way. However, some problems arise when using this ‘big particle’ approach: some values will become infinite during calculation and other variables need to be known for confining boundaries than for normal particles. The infinite inertia in fact prohibits the particles from influencing the boundary’s motion. The code can be written to handle these infinities, but it will be easier not to calculate the boundary’s equation of motion and simply externally imposing this motion. This however implies a distinct approach of boundaries and particles. Also the problem that for particles the centre’s position needs to be known and for boundaries their edge’s position and orientation, forces one to treat particles and boundaries in a different way.

#### 5. Simulation results

A simple 2D DEM code has been written to test this new approach. In the simulation circular particles are running through an inclined tube (Fig. 5). Apart from the problems arising from a lack of experience with DEM, one major problem showed up in the simulations. As can be seen in Fig. 3 the overlap between two pairs of particles is far too big. This is due to very large contact times when particles are rolling on each other: the particles remain in contact and so the end points of the contact-vector will rotate further away from each other, in the end making the overlap negative and therefore also the normal force will become negative. This means that particles will stick to each other and can even rotate inside each other (Fig. 6)!

Of course this is unacceptable. In order to avoid this problem the end points of the contact-vector would have to be renewed at each time step. This would cancel the advantage of deducing all forces from one single vector: the tangential force would then have to be calculated as an incremental force as the tangential component of the contact-vector will be set to zero at each time step. A lot of DE codes use this method.

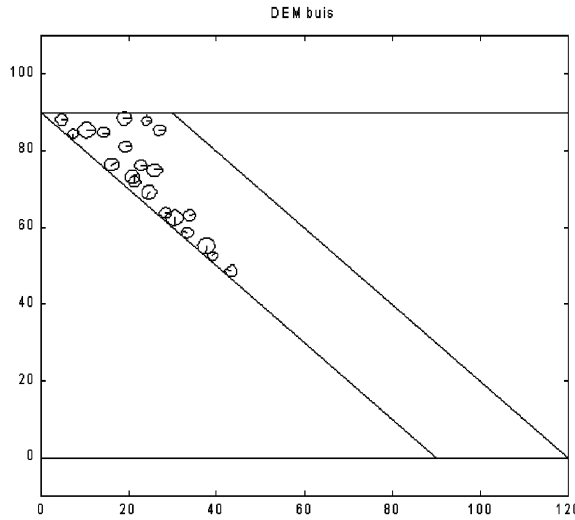


Fig. 5. DEM Simulation.

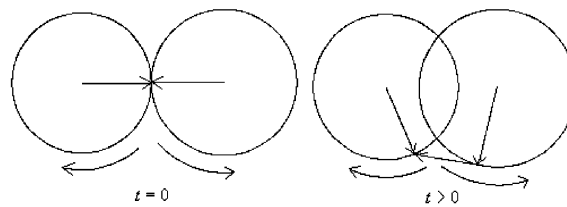


Fig. 6. Occurrence of unacceptable overlap.

**6. Conclusions**

The two-dimensional multibody approach has revealed some very small errors in the standard force equations used in the DEM. The thought experiment conducted showed that in special cases these errors could lead to significant differences in the calculated forces. In normal cases, however these differences will be negligible.

Treating boundaries as ‘large particles’ is theoretically possible, but the implementation of this approach was not possible unless treating these ‘large particles’ in a distinct manner and thus no advantage could be gained using this approach.

Computer simulations showed some problems with the contact-vector approach. To make it work properly the end points of the contact-vector should be renewed at each time step, but this would of course cancel the advantage of deducing all forces from one single vector.

**References**

[1] F. Pfeiffer, C. Glocker, *Multibody Dynamics with Unilateral Contacts*, Wiley, New York, 1996.

- [2] J.F. Favier, M.H. Abbaspour-Fard, M. Kremmer, A.O. Raji, Shape representation of axi-symmetrical, non-spherical particles in discrete element simulation using multi-element model particles, *Engineering Computations* 16 (1999) 467–480.
- [3] P.W. Cleary, N. Stokes, J. Hurley, Efficient collision detection for three dimensional super-ellipsoidal particles, in: *Proceedings of the Computational Techniques and Applications Conference (CTAC97)*, Adelaide, 1997.
- [4] F.C. Moon, *Applied Dynamics*, Wiley, New York, 1998.
- [5] K. van Staeyen, *Bewegingsvergelijkingen van botsende deeltjes: Theorie en simulatie*, Eindwerk Faculteit Landbouwkundige en Toegepaste Biologische Wetenschappen, Katholieke Universiteit Leuven, Juli 1999.
- [6] J. Schäfer, S. Dippel, D.E. Wolf, Force schemes in simulations of granular materials, *J. Phys. I. France* 6 (1996) 5–20.
- [7] C.R. Wassgren, *Vibration of Granular Materials*, Ph.D. Thesis, California Institute of Technology, 1997.